Brain, Behavior, and Immunity 76 (2019) 48–60

Contents lists available at ScienceDirect

Brain, Behavior, and Immunity

journal homepage: www.elsevier.com/locate/ybrbi

Chronic psychological stress impairs germinal center response by repressing miR-155

Weiguo Sun[a], Lingxia Zhang[a], Lejian Lin[b], Wei Wang[c], Yanhu Ge[d], Yanhua Liu[a], Bingfen Yang[a], Jianghou Hou[a], Xiaoxing Cheng[a], Xiaogang Chen[b], Zhongyuan Wang[a,*]

[a] Key Laboratory of Tuberculosis Prevention and Treatment of PLA, Division of Research, Institute of Tuberculosis, 309 Hospital, Beijing, China
[b] Department of Cardiovascular Diseases, 309 Hospital, Beijing, China
[c] Department of Neurology, 309 Hospital, Beijing, China
[d] Department of Anesthesiology, 309 Hospital, Beijing, China

ARTICLE INFO

Keywords:
Chronic psychological stress
Corticosterone
Germinal center
B cells
miR-155
FBXO11
BCL6

ABSTRACT

Germinal centers (GC) are vital to adaptive immunity. BCL6 and miR-155 are implicated in control of GC reaction and lymphomagenesis. FBXO11 causes BCL6 degradation through ubiquitination in B-cell lymphomas. Chronic psychological stress is known to drive immunosuppression. Corticosterone (CORT) is an adrenal hormone expressed in response to stress and can similarly impair immune functions. However, whether GC formation is disrupted by chronic psychological stress and its molecular mechanism remain to be elucidated. To address this issue, we established a GC formation model in vivo, and a GC B cell differentiation model in vitro. Comparing Naive B cells to GC B cells in vivo and in vitro, the differences of BCL6 and FBXO11 mRNA do not match the changes at the protein level and miR-155 levels that were observed. Next we demonstrated that CORT increase, induced by chronic psychological stress, reduced GC response, IgG1 antibody production and miR-155 level in vivo. The effect of chronic psychological stress can be blocked by a glucocorticoid receptor (GR) antagonist. Similarly, impaired GC B cell generation and isotope class switching were observed. Furthermore, we found that miR-155 and BCL6 expression were downregulated, but FBXO11 expression was upregulated in GC B cells treated with CORT in vitro. In addition, we demonstrated that miR-155 directly down-regulated FBXO11 expression by binding to its 3́-untranslated region. The subsequent overexpression of miR-155 significantly blocked the stress-induced impairment of GC response, due to changes in FBXO11 and BCL6 expression, as well as increased apoptosis in B cells both in vivo and in vitro. Our findings suggest perturbation of GC reaction may play a role in chronic psychological stress-induced immunosuppression through a glucocorticoid pathway, and miR-155-mediated post-transcriptional regulation of FBXO11 and BCL6 expression may contribute to the impaired GC response.

1. Introduction

The immune system is highly sensitive to stress. Positive benefits are apparent during acute incidences of stress such as increased drive. However chronic psychological stress may lead to negative physiological outcomes such as immunosuppression (Dhabhar, 2014; Aubert, 2008). Furthermore, chronic psychological stress has the potential to impair host antibacterial and antiviral defenses (Aberg et al., 2007; Steelman et al., 2009). Chronic psychological stress affects immune surveillance and is associated with a multitude of pathologies including tumor development and autoimmune diseases (Neeman and Ben-Eliyahu, 2013; McEwen, 2000). It is well established that chronic psychological stress leads to continuous activation of the hypothalamic-pituitaryadrenal (HPA) axis via increased sex hormone production including glucocorticoids (Haczku and Panettieri, 2010). Glucocorticoids, including endogenously produced corticosterone (CORT), can significantly affect both innate and adaptive immunity while simultaneously possessing immunosuppressive properties (Webster et al., 2002; Riccardi et al., 2002). Recent studies have identified immunosuppressive effects of increased plasma glucocorticoid levels, including impaired CTL responses (Truckenmiller et al., 2006), impaired DC maturation (Elftman et al., 2007), diminished B cell lymphopoiesis (Igarashi et al., 2005) and suppression of NK cell cytotoxicity (Rosenne et al., 2014). However, the exact processes underlying how chronic

* Corresponding author at: Division of Research, Institute of Tuberculosis, 309 Hospital, 17 Hei Shan Hu Road, HaiDian, Beijing 100091, China.
E-mail address: wzy2004177@sina.com (Z. Wang).

https://doi.org/10.1016/j.bbi.2018.11.002
Received 5 May 2018; Received in revised form 26 October 2018; Accepted 1 November 2018
Available online 08 November 2018
0889-1591/

psychological stress negatively impacts humoral immune responses (adaptive immunity, especially B lymphocytes development and differentiation) remain elusive.

B lymphocytes are critical players in the antibody production process which is maintained by humoral responses. Upon encountering an antigen, a differentiation and development process of Naive B cells generates or yields germinal center (GC) formation. GC is a characteristic histological structure in which B lymphocytes undergo clonal expansion, class switch recombination (CSR), somatic hypermutation, and affinity maturation before eventually differentiating to memory B cells and plasma cells (Suan et al., 2017; Klein and Dalla-Favera, 2008). Considerable effort has been made to investigate the mechanisms governing germinal center development.

BCL6 is a transcription factor that is vital for GC formation (Huang and Melnick, 2015; Basso and Dalla-Favera, 2012). BCL6 is expressed at much higher levels in GC B cells than in Naive B cells, and BCL6 is necessary for B cells to transition into GC B cells (Crotty et al., 2010). BCL6 expression is regulated by several signaling pathways at the transcriptional and protein level, and is essential for GC development. Recently, several observations have identified BCR and CD40 signaling pathways (Polo et al., 2008; Basso et al., 2004), NF-kB-mediated activation of IRF4 (Saito et al., 2007) and DNA damage promoted ATM (ataxia telangiectasia mutated) pathway (Phan et al., 2007) are involved in BCL6 regulation by the transcriptional downregulation or ubiquitin–proteasome pathway. Notably, a SKP1–CUL1–Fboxprotein (SCF) ubiquitin ligase complex that containing orphan F-box protein FBXO11 (Cardozo and Pagano, 2004) was revealed to display an ability to induce BCL6 ubiquitylation and degradation, mutations and deletions in FBXO11 can lead to lymphoma development because they stabilize BCL6 in Diffuse Large B Cell Lymphoma Cell Lines (DLBCLs) (Duan et al., 2012).

MicroRNAs (miRNAs) are small noncoding RNAs post transcriptionally regulating gene expression (Huntzinger and Izaurralde, 2011). MicroRNAs are necessary for many parts of B cell development and immune function, including GC responses (de Yebenes et al., 2013). To date very few miRNAs specifically linked to GC B cells have been identified (Schmidt and Küppers, 2014). One such example is miR-155, which is highly expressed in GC B cells, and regulates class switching, affinity maturation, and GC maintenance (Teng et al., 2008; Nakagawa et al., 2016; Rodriguez et al., 2007). Moreover, fewer GC B cells are present in miR-155 deficient mice, and its overexpression led to the opposite phenotype (Thai et al., 2007). However, it is not fully understood as to how miR-155 modulates GC responses at the molecular or cellular level.

In this study, we showed how chronic psychological stress suppressed GC response in vivo, and CORT prevented GC B cell differentiation in vitro. Additionally, CORT could prevent miR-155 expression, and result in FBXO11 increase and BCL6 reduction. These observations suggest that CORT inhibits miR-155 expression. Furthermore, miR-155 inhibition results in FBXO11 up-regulation, which yields increased degradation of BCL6 in B cells and apoptosis of GC B cells via ubiquition. Finally, we revealed a mechanism in impaired GC response caused by chronic psychological stress.

2. Materials and Methods

2.1. Chronic psychological stress

Male C57BL/6 mice, between 6 and 8 weeks old were purchased from the Institute of Experimental Animals, Academy of Chinese Medical Sciences. Six mice per cage were housed in accordance with the care and use of laboratory animal manual standards established by the 309 Hospital in specific pathogen free conditions. For restraint, mice were held in a 50 ml conical tube with ventilation holes. They were restrained for 12 consecutive nights corresponding to the normal active day period. After 12 h of horizontal restraint, mice were given 12 h to rest with food and water ad libitum. Control mice were not restrained, and had access to food and water only during the same period as the restrained mice. To assess glucocorticoid function, mice were subcutaneously injected with 25 mg/kg RU486, or vehicle control (ichel propylene glycol/ethanol (7/3 v/v)) for 12 days. RU486 was injected 1 h before stress period.

2.2. Immunization

C57BL/6 mice (8 weeks, female, 6 mice/group) were immunized via i.p. injection with 100 μg alum-precipitated chicken gamma-globulin conjugated (4-hydroxy-3-nitrophenyl) acetyl (NP-CGG) (Biosearch Technologies). NP-CGG was injected 2 h before stress period. Twelve days after immunization and restraint stress, mice were sacrificed for GC response and Ab production analyses. Splenic GC response was analyzed by immunohistochemistry and flow cytometry. Retro-orbital bleeding was used to collect blood for serum preparation at appropriate time points.

2.3. Immunofluorescence and histological analysis

Fresh spleen was fixed in 4% PFA overnight and then was sectioned. Frozen sections were rinsed with PBS once for 5 min to remove the OCT. Block with 3% normal donkey serum (NDS) in PBS at room temperature (RT) for 30 min. Incubate with primary antibodies diluted in 3% NDS/PBS at 4 °C overnight. The primary antibodies: Rat anti-GL-7 (eBioscience) for GC B cells, Rabbit anti-CD3 (Dako) for T cells. Negative control was blotted with 3% NDS/PBS only. Wash sections with PBS 3 times for 5 min each. Add secondary antibodies (diluted with 3% NDS/PBS) to each section and incubate for 1 h at RT avoid light. Blot with the following secondary antibodies: FITC-donkey anti-rat IgG (Invitrogen), PE-donkey anti-rabbit IgG (Invitrogen). Remove secondary antibodies and wash with PBS for 3 times (5 min each time). Add DAPI (Sigma, 1:1000 diluted) to each section and incubate for several minutes. Wash sections with PBS for 5 min and repeat 3 times. A fluorescence microscope was used to analyze stained tissue sections (Eclipse E400; Nikon). Sections were blinded and quantification was conducted using the IPLab 4.0 software. GC number and size were quantitated by morphometric analysis of $GL7^+$ staining. GC number and size, were measured in arbitrary units based on the number of positively stained pixels, and averaged for all splenic $GL7^+$ clusters from 3 control or treated mice.

2.4. FACS analysis and sorting

Cell suspensions from mouse spleen and in vitro cell cultures were prepared and stained according to established protocols. The following reagents were used to stain cells for FACS analysis and sorting (all from BD Biosciences unless otherwise indicated): B220-PerCP, GL7-APC (eBioscience) and Fas-FITC for germinal center B cells phenotype screen; B220-PerCP, IgG1-FITC (eBioscience) and IgM-PE for class switch screen. B220-PerCP, CD69-PE, GL7-APC (eBioscience) and Fas-FITC for Naive B cells ($B220^+CD69^-GL7^-Fas^-$ populations) and GC B cells ($B220^+CD69^-GL7^+Fas^+$ populations) sorting.

2.5. Immunoblot analysis

Cells were lysed and run on a 12% SDS-PAGE gel. Protein was transferred to polyvinylidene difluoride membranes (Polyscreen; PerkinElmer) with a mini Trans-Blot apparatus (Bio-Rad). Membranes were blocked for 2 h, and then were blotted with primary antibodies [anti-BCL6 (BD Biosciences), anti-FBXO11 (Santa Cruz Biotechnology) or anti-mouse β-actin (Sigma-Aldrich)] at 4 °C for overnight. Then HRP-conjugated secondary Abs were used to probe the blot for 1 h at RT, and protein levels were visualized using ECL substrate (Pierce Chemical).

2.6. Quantitative real-time PCR

Total RNA was isolated using TRIZOL Reagent (Invitrogen) according to manufacturer's protocol. Total RNA (1 μg) was reverse transcribed to cDNA using Superscript First Strand Synthesis RT-PCR System (Invitrogen). cDNA was then used at a 1:100 dilution ratio as a PCR template for amplification as recommended by the manufacturer. SYBR Green PCR Master Mix (Applied Biosystems) was used for real time RNA detection with the following primers: BCL6 forward 5′-CAG CAACATCTACTCGCCCAA-3′ and

BCL6 reverse 5′-ATGGAGCATTCCGAGCAGAAG-3′,
FBXO11 forward 5′-GGCGAGAGGGATGATGTTCC-3′ and
FBXO11 reverse 5′-TCTGCGAAGTTGGTATGGACTAT-3′,
GAPDH forward 5′-GAAGGTGAAGGTCGGAGTC-3′ and
GAPDH reverse 5′-GAAGATGGTGATGGGATTTC-3′.

For miRNA isolation, the miRNA easy mini kit (Qiagen) was used. cDNA synthesis was completed with the miScript II RT kit (Qiagen) according to the manufacturer's instructions. A miR-155-5p specific primer was used for qPCR detection of miR-155-5p using the miScript SYBER Green PCR kit (Qiagen). A ROTOR-GENE Q (Qiagen) was used for the qPCR reaction. Melt curve analysis was used to confirm primer specificity.

2.7. Measurement of serum Ab

Anti-NP hapten antibody was checked by ELISA using plates that were coated with NP-BSA. Briefly, 96 well plates (Falcon; Becton Dickinson, Oxnard, CA) were incubated with 2.5 μg NP_{16}-BSA (N-5050–100, Biosearch Tech Inc.) overnight at 4 °C. Plates were washed twice with wash buffer (0.05% Tween-20 in 1X PBS) and then blocked with 200 μl 1% BSA in PBS for 1 h at RT. 100 μl of mouse serum from immunized mice or control mice were added to the plate and incubated at RT for 2 h. Plates were washed with PBS containing 0.05% Tween 20, and HRP-rat anti-mouse IgG or IgM were added to the plate with a dilution of 1:750, diluted with 1% BSA in PBS. After washing, add 100 μl of substrate solution and when desired, terminate the reaction with 50 μl of Stop Solution. Absorbance at 450 nm was assessed using a microplate reader.

2.8. B lymphocyte isolation and induced germinal center B cells culture

In-vitro-induced GC B (iGC B) cells culture was modified from the protocol as described in Takuya Nojima's study (Nojima et al., 2011). Magnetic separation was used to isolate $CD43^-$ naïve splenic B lymphocytes (MACS, MiltenyiBiotec). Cell culture plates were coated with 1 μg/ml or 5 μg/ml mCD40L (eBioscience) for 2–3 h, the Naive B cells were maintained at 1–2 × 10^5/ml in culture medium, and treated with 100 ng/ml BAFF and 100 ng/ml IL4 to induce germinal center B cells. Cells were collected for FACS, RNA isolation, or protein analysis at different time points.

2.9. Corticosterone treatment in vitro

The corticosterone (Sigma-Aldrich) was dissolved in DMSO to a concentration of 1 mM. Naive B cells suspension was treated with corticosterone solution in a dose of 1 μM at the beginning of cells culture. DMSO (0.1%) was delivered as the vehicle control.

2.10. Measurement of Ab

Naive B cells were treated with a cytokine cocktail for 3 days. The supernatant was gathered for total IgG or IgM quantification by sandwich ELISA. Experiment details are in the guidelines for mouse IgG/IgM ELISA (MABTECH). Coat a high protein binding ELISA plate with 1 μg/ml of anti-IgG/IgM antibody (100 μl/well), dilute in PBS, pH 7.4. Incubate overnight at 4–8 °C. Wash twice with PBS (200 μl/well). Block with 200 μl/well of 0.1% BSA in PBS with 0.05% Tween 20 (PBST). Incubate for 1 h at RT and wash with PBST 5 times. Add 100 μl/well of samples or standard and incubate for 2 h at room temperature. Wash 5 times with PBS-Tween. Add 100 μl/well of anti-IgG/IgM-ALP. Incubate for 1 h at RT and then wash with PBST 5 times. Add 100 μl/well of appropriate substrate. Measure absorbance at 405 nm using a plate reader after suitable developing time.

2.11. Luciferase reporter assay

The 3′-UTR of FBXO11 mRNA containing the miR-155 binding site was cloned into pcDNA3.1-luc, pcDNA3.1-Luc-wtUTR. A mutated pcDNA3.1-Luc-muUTR FBXO11 reporter plasmid was made by mutating miR-155 binding sites via site-directed mutagenesis according to the manufacturer's protocol (Stratagene). For reporter gene binding assays, 293 T cells were transfected with using pcDNA3.1-Luc-wtUTR and pcDNA3.1-Luc-muUTR as well as with miR-155 mimics (Genepharma, China). The pSV40-Renilla plasmid was used as a control. After 24 hr, the ratio of luciferase to Renilla was assessed using a dual luciferase reporter gene kit (Promega).

2.12. Cell culture and transfection

Su-DHL4 cells (5 × 10^5 cells/ml) were grown in a 5% CO_2 humidified environment in RPMI 1640 medium (Gibco, Grand Island, NY, USA) containing 10% heat-inactivated Fetal Calf Serum (FCS), 100 U/ml penicillin, 100 μg/ml streptomycin and 2 mM L-glutamine (Gibco) at 37 °C. Cells were grown overnight and transfected with either hsa-miR-155 mimic, or negative control miRNA (Genepharma, China) using Lipofectamine 2000 (Invitrogen, USA). Oligonucleotide sequences were:

hsa-miR-155 mimic:
Sense: 5′-UUAAUGCUAAUCGUGAUAGGGGU-3′,
Antisense: 5′-CCCUAUCACGAUUAGCAUUAAUU-3′.
Negative control:
Sense: 5′-UUCUCCGAACGUGUCACGUTT-3′,
Antisense: 5′-ACGUGACACGUUCGGAGAATT-3′.

2.13. Lentiviral experiments

To overexpress miR-155 in Naive B cells, lentivirus was generated using the BLOCK-iT Lentiviral Pol II miR RNAi expression system (Invitrogen). The pre-miR-155 and its reverse complement were annealed and ligated into the pcDNA6.2-GW/EmGFP-miR vector. After sequence verification, BP/LR Gateway recombination reactions were used to transfer the EmGFP-pre-miR-155 into to the pLenti6/V5 expression construct. The pLenti6/EmGFP–miR-155 vector was transfected into 293FT to generate viral particles. Naive B cells (1 × 10^5) were activated 24 h before incubation with LV-miR-155. Two days after infection, the cells were tested for iGC B cell production using FACS staining. Eight weeks old female C57BL/6 mice were infected with lentiviral particles via tail vein injection to overexpress miR-155 in spleen. After tail vein injections, the mice were treated with chronic restraint stress and immunization. The animals were sacrificed and the spleens were harvested for analyses 12 days posttreatment. All animal experiments were approved by the Animal Ethics Committee of the 309 Hospital, and conducted based on the Guide for the Care and Use of Laboratory Animals from the US National Institutes of Health (NIH Publication number 85-23, revised 2011).

2.14. Apoptosis analysis with annexin V

Splenocytes or B cells in vitro model were washed twice with cold PBS, resuspended in 100 μl annexin V buffer (Becton Dickinson) to 1 × 10^5 cells and then incubated for 15 min at RT. Apoptosis of B cells ($B220^+$) was analyzed subsequently using a FACS Aria machine (BD

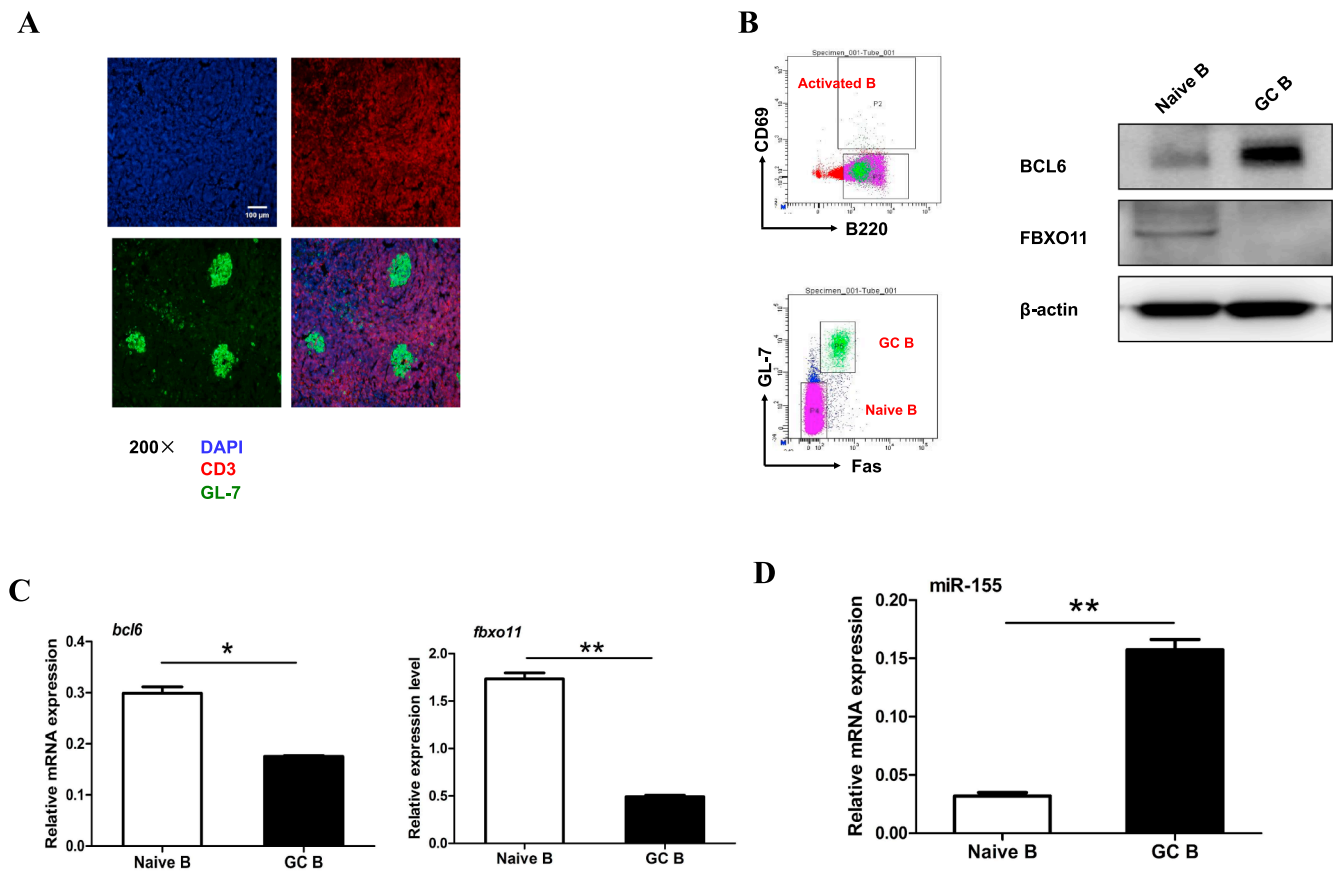

Fig. 1. Expression of BCL6, FBXO11 and miR-155 in the germinal center formation process. (A) GCs were observed in immunized mice. Spleens from C57BL/6 mice were collected on day 12 after immunization with NP-CGG. Splenic sections were stained for CD3 (T cell markers) in red, GL-7 (GC markers) in green, and DAPI in blue. Representative images of three animals per group were shown. Original magnification, ×200. (B) BCL6 expression was significantly upregulated in GC B cells compared with Naive B cells. Conversely, FBXO11 expression was significantly downregulated in GC B cells compared with Naive B cells. GC B cells were isolated from mice splenocytes by FACS sorting. First gated by $B220^{+}CD69^{-}$ for inactivated B cells, and further divided by $GL7^{+}Fas^{+}$ for GC B cells or $GL\text{-}7^{-}Fas^{-}$ for Naive B cells. Whole cell extracts from GC B cells and Naive B cells were analyzed by Western blotting with antibodies to BCL6, FBXO11 and β-actin. Representative images of three independent experiments were shown. (C) mRNA expression of BCL6 and FBXO11 were significantly downregulated in GC B cells compared with Naive B cells. mRNA levels were analyzed by real-time PCR. Data are mean ± SEM of three independent experiments. Asterisks represent statistical differences between groups; $*p < 0.05$. $**p < 0.01$ (D) Expression of miR-155 was significantly upregulated in GC B cells compared with Naive B cells. Expression of miR-155 was analyzed by real-time PCR. Data are mean ± SEM of three independent experiments. Asterisks represent statistical differences between groups; $**p < 0.01$. (For interpretation of the references to colour in this figure legend, the reader is referred to the web version of this article.)

Biosciences).

2.15. Statistical analyses

Data are represented as mean ± SEM. First, a one-way ANOVA was used to decide whether an overall statistically significant change occurred. Bonferronni's multiple-comparison test was used to analyze the differences between all groups. p values < 0.05 (*), 0.01 (**), and 0.001 (***) were considered statistically significant.

3. Results

3.1. miR-155, BCL6 and FBXO11 expression in GC B cells

To investigate the role of miR-155 in GC response, we immunized C57BL/6 mice with chicken-globulin (CGG) conjugated (4-hydroxy-3-nitrophenyl) acetyl (NP). Spleens were harvested for immunofluorescence staining and FACS analyses after 12 days. Mice developed morphologically normal splenic GC in response to NP-CGG immunization (Fig. 1A). To study the role of BCL6 and FBXO11 in GC formation, we FACS sorted Naive B cells and GC B cells from immunized mice's splenocytes. BCL6 was increased in CG B cell comparing to Naive B cells while FBXO11 was decreased (Fig. 1B). However, both BCL6 and FBXO11 mRNA levels were downregulated in GC B cells compared to their naïve counterparts (Fig. 1C). However, miR-155 expression level was significantly upregulated in GC B cells (Fig. 1D).

The above observations agree with the hypothesis that protein levels of BCL6 and FXBO11 are independently regulated regardless of mRNA expression. In addition, we observed increased levels of miR-155 in GC B cells in relative to Naive B cells. This result was consistent with the finding that reduced number of GC B cells compromised affinity maturation in miR-155-deficient B cells (Rodriguez et al., 2007; Thai et al., 2007).

3.2. Restraint stress treatment inhibits germinal center response and this inhibition is blocked by corticoid receptor antagonist RU-486

To investigate the mechanism of stress induced immune system alteration, we studied GC response in mice treated with a restraint stress. After twelve days post-immunization and introduction of a restraint stress, the mice were sacrificed for GC and Ab analyses. To determine whether plasma CORT can alter the GC response induced by chronic restraint stress, plasma from control and restrained animals was collected and analyzed. Plasma CORT level is elevated in restraint stress treated mice compared to control mice (Fig. 2A). Spleen GC response was analyzed by immunofluorescence staining and flow cytometry.

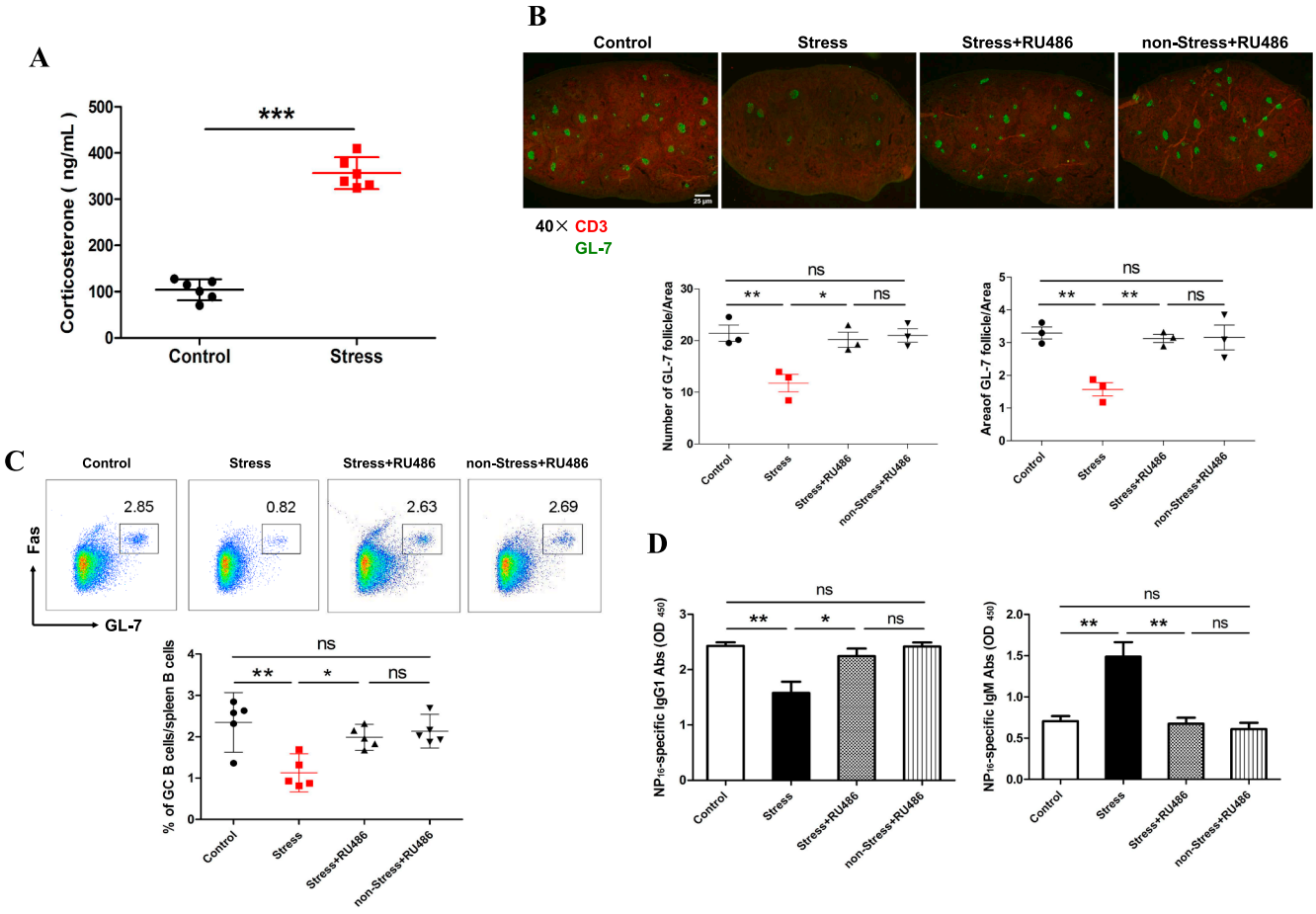

Fig. 2. Effect of chronic psychological stress on germinal center response in vivo. (A) Chronic restraint stress significantly enhanced plasma CORT levels in immunized mice. Mice (8 weeks-old, female, C57BL/6) were stressed following immunization with NP-CGG as described in Materials and Methods. On day 12, plasma was collected from stressed or unstressed (control) mice. The concentration of plasma CORT was determined by RIA. Each symbol represents one mouse and the horizontal bar corresponds to the media. Asterisks represent statistical differences between groups; $^{***}p < 0.001$. (B) Chronic psychological stress significantly suppressed the ratio of GC number and size to spleen area in immunized mice and which was significantly reversed by treatment with RU-486. On day 12, mice in each group were sacrificed. Each spleen was collected and was analyzed by immunofluorescence. Graphical representation of GC stained green as described in *Materials and Methods.* GC number and size to spleen area were quantitated by morphometric analysis of GL-7$^+$ staining on IHC. Representative images are shown. Original magnification, ×40. Each symbol represents one mouse and the horizontal bar corresponds to the media. Asterisks represent statistical differences between groups; $^{**}p < 0.01$. (C) Chronic psychological stress significantly suppressed the GC B cells proportion of spleen B cells in immunized mice and was significantly reversed by treatment with RU-486. Splenocytes were prepared aseptically from each group. The percentages of GC B cells out of splenic B cells were assessed by co-staining with anti-GL-7 and anti-Fas Abs after gated by anti-B220 Abs. Representative images are shown. Percentages of cells in each quadrant are indicated. Each symbol represents one mouse and the horizontal bar corresponds to the media. Asterisks represent statistical differences between groups; $^{*}p < 0.05$; $^{**}p < 0.01$. (D) Chronic psychological stress mice demonstrated a significant reduction in NP_{16}-specific IgG1 antibody titers and a significant increase in NP_{16}-specific IgM, which were significantly reversed by treatment with RU-486. NP-specific antibody titers were measured in sera of each group as described in *Materials and Methods*. All sera were diluted 1:25,000. The data represent the mean ± SEM from six individual mice in each group. Asterisks represent statistical differences between groups; $^{**}p < 0.01$. (For interpretation of the references to colour in this figure legend, the reader is referred to the web version of this article.)

Interestingly, GC response was significantly decreased in stressed mice compared to control mice. Both GC size and frequency were reduced in the spleens of stressed animals which were blocked by Ru486. However, no significant changes in GC size and frequency were observed between RU486 treated controls and non-treated controls (Fig. 2B). Consistently, flow cytometry demonstrated that GC B-cell population (GL-7$^+$Fas$^+$) was significantly smaller in stressed mice (Fig. 2C), and RU-486 significantly blocked this effect. But no significant changes in GC B-cell population were observed between RU-486 treated controls and non-treated controls. To study the functional consequence of stress induced inhibition of GC response, we measured the production of (IgM) NP-specific Ab levels and class-switched (IgG1) NP-specific Ab levels in stressed mice and control mice. Our data confirmed a significant reduction of class switched NP-specific IgG1 Ab production in stressed mice relative to control mice, and significant increase of NP-specific IgM Ab levels were observed in stressed mice. Treatment with RU-486 significantly inhibited this effect, whereas no differences were seen in NP-specific IgM or IgG1 Ab between RU486 treated controls and non-treated controls (Fig. 2D).

To determine the effect of stress on in vivo miR-155 levels, mi-155 expression was measured via quantitative PCR in B lymphocytes isolated from mice spleen. We found stress exposure significantly repressed the expression of miR-155 in spleen B cells. Treatment with RU-486 significantly inhibited this effect, but no significant changes were observed in miR-155 expression between RU-486 treated control and non-treated control (Supplement Fig.).

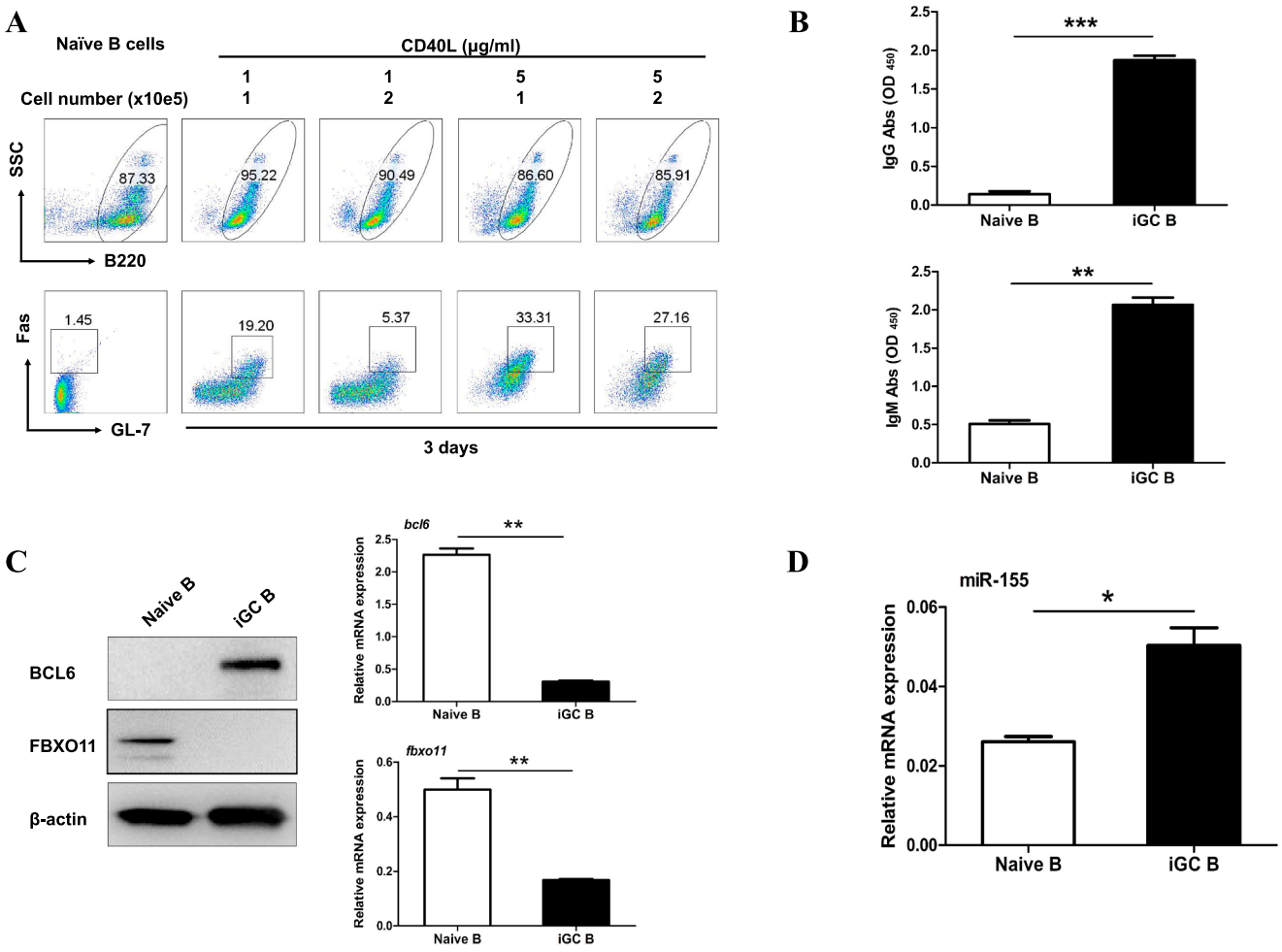

Fig. 3. In vitro induction of phenotypically GC B cells from naive B cells. (A) Naive B cells were treated with CD40 ligand, IL4 and BAFF to induce it differentiated into GC B cells in vitro. Coating cell culture plates with mCD40L (1 μg/ml, 5 μg/ml) for 2–3 h, 100 μl Naive B cell suspension (1×10^5, 2×10^5 cells) and 100 μl cytokines' cocktail (BAFF 200 ng/ml + IL4 200 ng/ml) were added into each well. FACS staining was used for converted GC B cells ($B220^+$ $GL\text{-}7^+$ Fas^+) screening after culture in CO_2 incubator for 3 days. Representative images were shown. Percentages of cells in each quadrant were indicated. **(B)** IgG and IgM levels were significantly elevated in supernatant of iGC B cells compared with Naive B cells. IgG and IgM antibodies in supernatant of iGC B cells were detected by ELISA. The data represent the mean ± SEM from six independent experiments. Asterisks represent statistical differences between groups; $^{**}p < 0.01$; $^{***}p < 0.001$. **(C)** Expression of BCL6 protein was significantly upregulated but BCL6 mRNA level was largely downregulated in iGC B cells compared with Naive B cells. Expression of FBXO11 mRNA and protein were all significantly downregulated in iGC B cells compared with Naive B cells. Whole cell extracts from Naive B cells or iGC B cells were analyzed by Western blotting with antibodies to BCL6, FBXO11 and β-actin. Representative images of three independent experiments were shown. The data represent the mean ± SEM from six independent experiments. Asterisks represent statistical differences between groups; $^{**}p < 0.01$. **(D)** miR-155 level was significantly upregulated in iGC B cells compared with Naive B cells. Expression of miR-155 in aforementioned cells was analyzed by real-time PCR. Data (mean ± SEM) were obtained from six independent experiments. Asterisks represent statistical differences between groups; $^{*}p < 0.05$.

3.3. Generation of GC phenotype B cells in vitro

To study how CORT affects GC B cell differentiation in vitro, we cultured naïve splenic B cells by co-stimulation with CD40L, BAFF and IL-4 to induce GC phenotypic B cells. The phenotype of the induced B cells was analyzed by flow cytometry. As expected, the $B220^+$ cells exhibited a GC B cell-surface phenotype: $GL7^+$ Fas^+ (Fig. 3A). These indicated that 1×10^5B cell number, 5 μg/ml CD40L stimulating dose and 3 days culture time were required for optimum induction of B cells to a GC phenotype. Consistent with the GC B cells, IgG and IgM antibody levels were significantly elevated in iGC B cells in relative to Naive B controls (Fig. 3B), suggesting that iGC B cells undergo Immunoglobulin class switch recombination.

To delineate the molecular mechanism that underlying the observed iGC B cells differentiation, we checked the expression level of BCL6, FBXO11 and miR-155. As shown in Fig. 3C, BCL6 and FBXO11 mRNA levels were significantly reduced in iGC B cells. While BCL6 protein was increased in iGC B cells, and FBXO11 protein level was significantly downregulated compared with Naive B cells. Consistently, miR-155 levels were significantly elevated in iGC B cells. These findings are in agreement with the in vivo model and indicate BCL6 and FBXO11 expression by miR-155 involve iGC B cell generation.

3.4. In vitro GC B cells differentiation were impaired by corticosterone (CORT)

Low levels of CORT are constitutively produced in vivo, but they are upregulated in response to stress. Higher levels of CORT act by binding to the glucocorticoid receptor (GR). To determine how CORT affects the generation of GC B cells, we treated cultured Naive B cells with CORT (1 μM) for 72 h. The CORT concentration used was comparable to that observed in mice responding to stress (Median, 347 ng/ml, approximately 1 μM). The population of GC B cells ($GL7^+$ Fas^+) and CSR phenotypes (IgM^- $IgG1^+$) in cell culture treated with CORT were significantly reduced compared with iGC B cells group (Fig. 4A). We further addressed whether BCL6, FBXO11 and miR-155 were required for

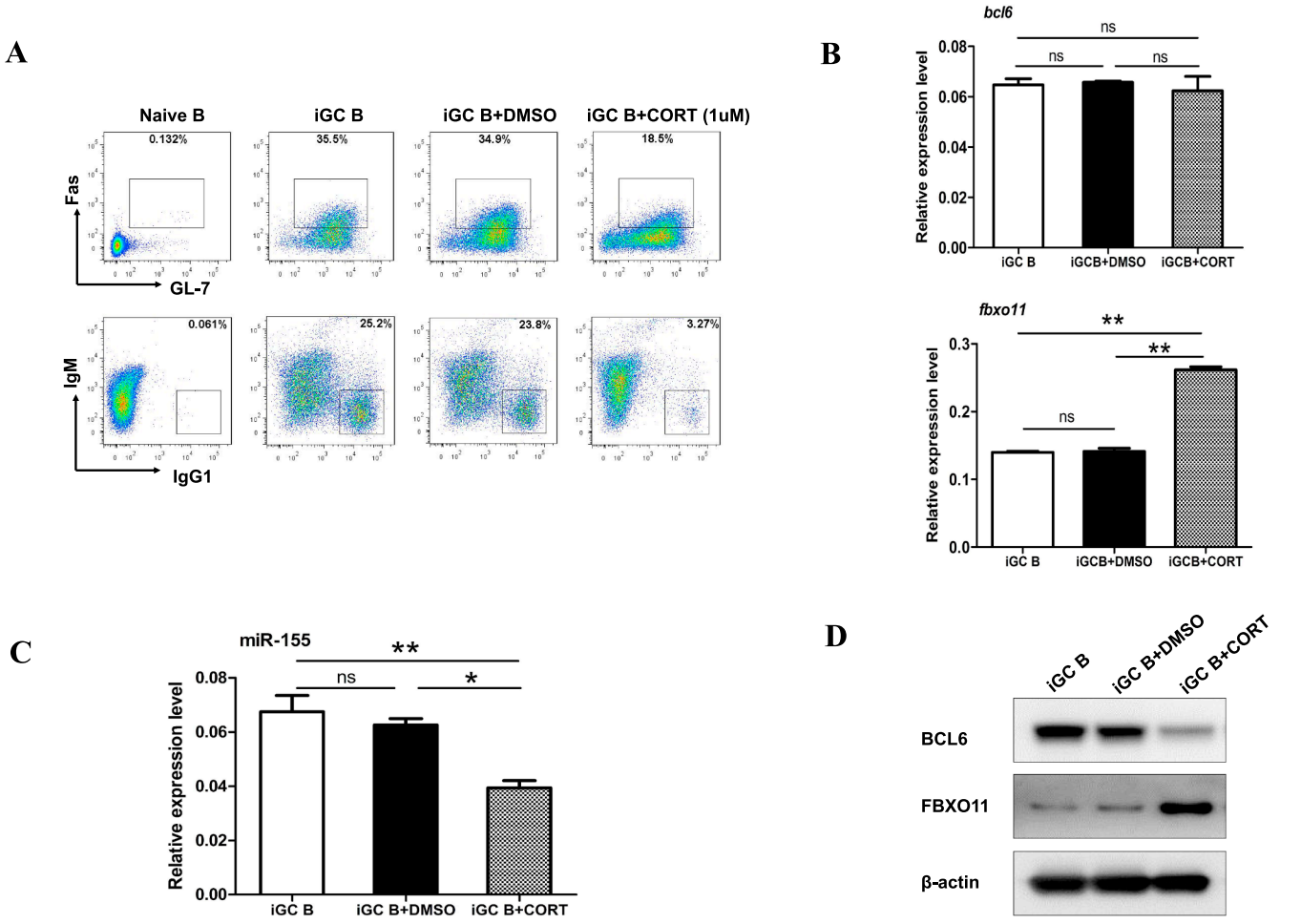

Fig. 4. Effects of CORT treatment on iGC B cells differentiation in vitro. (A) CORT (1 μM) suppressed differentiation of Naive B cells to iGC B cells and immunoglobulin class switching. DMSO had no effect on iGC B cells differentiation and immunoglobulin class switching. FACS staining of induced GC B cells (GL-7$^+$ Fas$^+$) and IgG1-switched cells (IgG1$^+$ IgM$^-$) were obtained from the following groups: Naive B cells, iGC B cells, iGC B cells + DMSO, iGC B cells + CORT (1 μM). Representative images are shown. **(B)** CORT significantly enhanced FBXO11 mRNA expression in Naive B cells during its differentiation into iGC B cells. CORT had no effect on BCL6 mRNA expression in B cells. DMSO had no effect on BCL6 and FBXO11 mRNA expression in B cells. Expression of BCL6 and FBXO11 mRNA was assessed by q-PCR. Data are mean ± SEM of six independent experiments; $^{**}p < 0.01$. **(C)** CORT significantly suppressed miR-155 expression in Naive B cells during its differentiation into iGC B cells. DMSO treatment had no effect on miR-155 expression. Expression of miR-155 was assessed by q-PCR. Data are mean ± SEM of six independent experiments; $^{*}p < 0.05$; $^{**}p < 0.01$. (D) The enhanced FBXO11 expression of Naive B cells during its differentiation into iGC B cells through CORT (1 μM) treatment was detected. The significant reduction of BCL6 expression in Naive B cells treated with CORT was also observed which might associated with increased FBXO11 expression. DMSO treatment had no effect on BCL6 or FBXO11 expression. Whole cell extracts from 3 days of cell cultures were analyzed by Western blotting with antibodies to BCL6, FBXO11 and β-actin. Representative images of three independent experiments were shown.

impairment of iGC B cell generation. CORT treatment significantly increased FBXO11 mRNA level, but had no substantial change in BCL6 mRNA level (Fig. 4B). Compared to iGC B cells, CORT treatment significantly reduced miR-155 expression (Fig. 4C). However, BCL6 protein level was downregulated, and FBXO11 protein level was upregulated in iGC B cells treated with CORT (Fig. 4D). In contrast, this effect was not affected by DMSO. Thus, our data suggest that CORT impairs GC B cells differentiation through regulation of miR-155, FBXO11 and BCL6.

3.5. miR-155 target the 3′UTR of FBXO11

Since miR-155 level was negatively correlated with the expression of FBXO11, we speculated that miR-155 regulates FBXO11 expression. We identified a putative miR-155 binding site on murine FBXO11 using TargetScan., We confirmed mmu-miR-155 target the 3′UTR of FBXO11 using luciferase reporter assays. Mutation of the predicted binding sites abolished the suppression by mmu-miR-155 (Fig. 5A). We analyzed miR-155 expression in Su-DHL4 cells transfected with hsa-miR-155 or negative control. As shown in Fig. 5B, we detected significantly more miR-155 expression in Su-DHL4 cells transfected with hsa-miR-155 than those transfected with a negative control. FBXO11 mRNA and protein level in hsa-miR-155 transfected Su-DHL4 cells were significantly less than in negative control transfected cells (Fig. 5C, D), suggesting miR-155 regulates FBXO11 expression.

3.6. Overexpressing miR-155 blocks CORT's inhibition of iGC B cells differentiation

The data described above suggests that miR-155 could target FBXO11. Since iGC B cells differentiation was inhibited by CORT, we attempted to determine the influence of miR-155 overexpression on CORT using a lentiviral system. We found miR-155 overexpression significantly blocked the reduction of miR-155 levels in iGC B cells treated with CORT (Fig. 6A). The CORT induced reduction of GC phenotype B cells (GL-7$^+$Fas$^+$) were significantly inhibited by miR-155 (Fig. 6B). CORT treatment on miR-155 transfectant did not affect BCL6 mRNA level, but miR-155 overexpression blocked CORT treatment

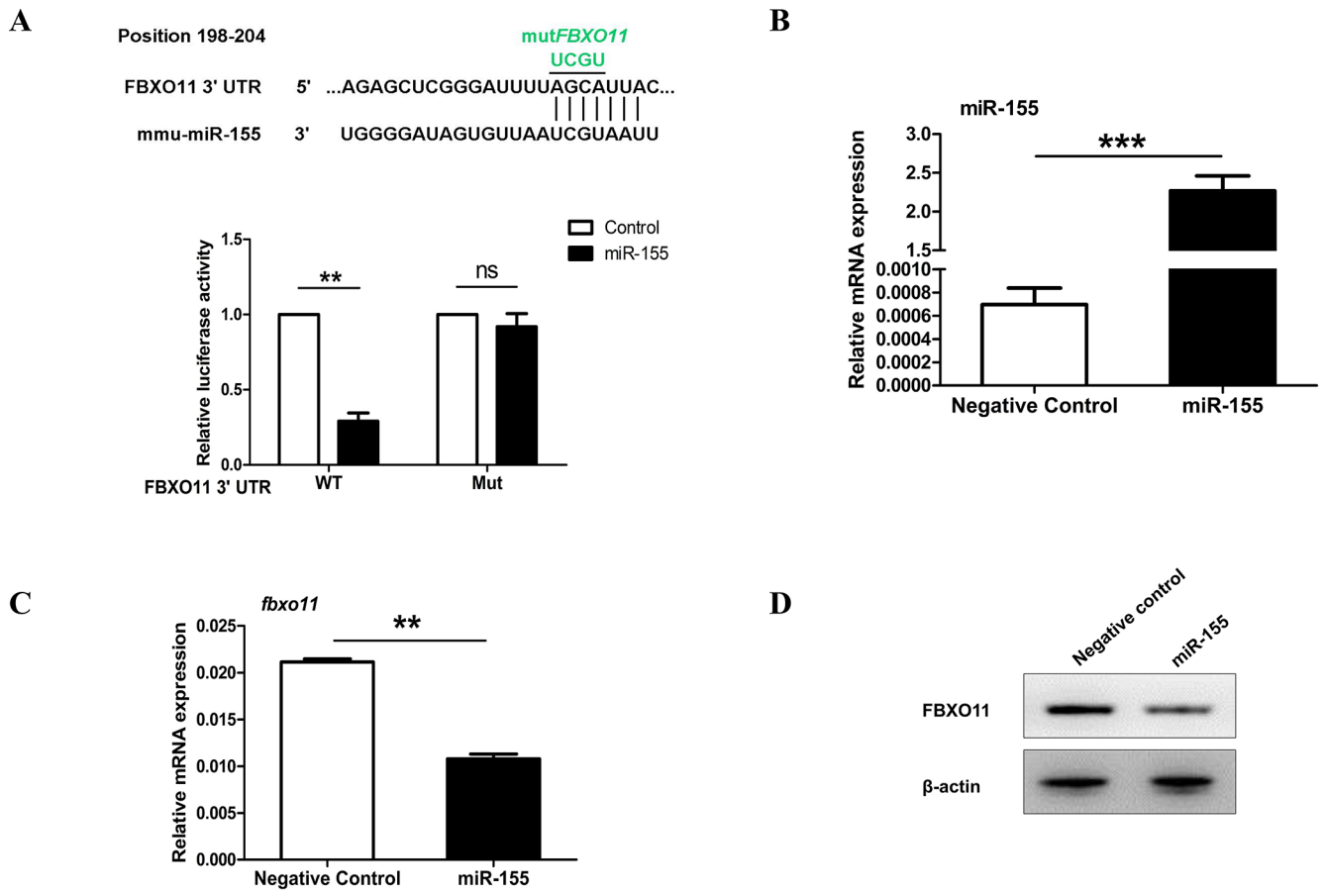

Fig.5. 3′ UTR of FBXO11 is a direct target of miR-155 and its overexpression in DLBCL cell lines results in a reduction of FBXO11 expression. (A) Potential miR-155 targeting sites in the 3′UTR of murine FBXO11 mRNA (Position 198–204) predicted by TargetScan were mutated. HEK293T cells were co-transfected with mmu-miR-155 mimics and pcDNA3.1-luc vector containing the FBXO11 3′ UTR or the FBXO11 3′ UTR with mutations in predicted miR-155 binding site. They were assessed for luciferase activity at 24 h after transfection. Data are mean ± SEM of three independent experiments. Significant difference was observed; $^{**}p < 0.01$. **(B)** Su-DHL4 cells were transfected with hsa-miR-155 or control miRNA. Data are mean ± SEM of three independent experiments. Significant difference was observed; $^{***}p < 0.001$. **(C)** Significant downregulation of FBXO11 mRNA level was found in Su-DHL4 cells transfected with hsa-miR-155 compared with control miRNA. Data are mean ± SEM of three independent experiments. Significant difference was observed; $^{**}p < 0.01$. **(D)** FBXO11 protein levels were largely downregulated in Su-DHL4 cells transfected with hsa-miR-155. Whole cell extracts from Su-DHL4 cells at 48 h post transfection were analyzed by Western blotting with antibodies to FBXO11 and β-actin. Representative images of three independent experiments were shown.

induced upregulation of FBXO11 (Fig. 6C). CORT treatment decreased BCL6 protein level, but increased FBXO11 protein level in iGCB cells. MiR-155 transfection of differentiated iGC B cells significantly blocked CORT-induced reduction of BCL6 protein and increased FBXO11 protein (Fig. 6D). Consistent with BCL6 protein expression level changing, we found that miR-155 transfection significantly blocked apoptosis in B cells induced by CORT (Fig. 6E). These results demonstrate that miR-155 controls GC B cell differentiation through the regulation of FBXO11 expression during the stress hormones stimulation.

3.7. Overexpressing miR-155 blocks restraint stress's induced impairment of GC response in mice

To investigate the role of miR-155 in vivo, mice were administered lentiviral particles containing pre-miR-155 via tail vein injections before immunization and chronic restraint stress. Stressed animals have less GC B-cell population ($GL\text{-}7^{+}Fas^{+}$) in contrast to the control group. This reduction was blocked by miR-155 overexpression (Fig. 7A). Same as the in vitro model, miR-155 overexpression significantly altered the stress-induced reduction of miR-155 level in spleen B cells (Fig. 7B). Furthermore, miR-155 overexpression blocked the stress-induced increase of FBXO11 expression, while it did not alter BCL6 mRNA levels in spleen B cells (Fig. 7C). MiR-155 overexpression in mice significantly inhibited stress-induced upregulation of FBXO11 protein, and blocked the stress-induced reduction in the BCL6 expression (Fig. 7D). Consistently, we found that miR-155 overexpression in mice significantly inhibited the increase of apoptosis in spleen B cells induced by stress (Fig. 7E). These findings suggest that miR-155 acts through targeting FBXO11 expression and regulates BCL6 levels indirectly to reverse the immunosuppressive effects induced by stress.

4. Discussion

Our studies suggest that chronic, restraint stress has immunosuppressive effects through impairment of GC response. This is supported by both in vivo and in vitro results that CORT is an important chronic psychological stress hormone and is responsible for the GC B cells apoptosis. Our study disclosed the molecular mechanism of how

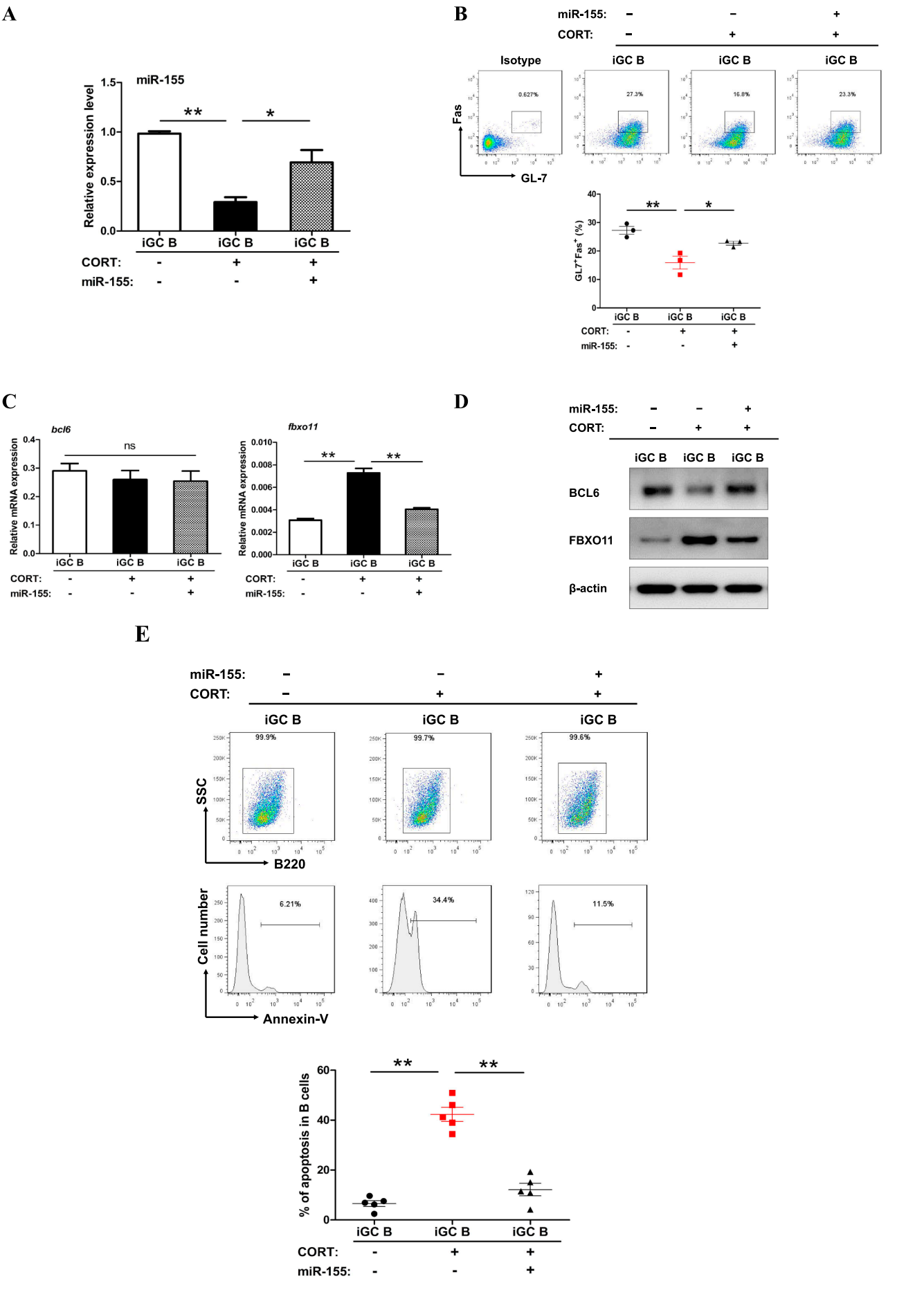

(caption on next page)

Fig.6. Effects of miR-155 on iGC B cells differentiation treated with CORT. (A) Overexpression of miR-155 prevented miR-155 reduction in Naive B cells during its differentiation into iGC B cells thorugh CORT treatment (1 μM). Expression of miR-155 in iGC B cells, with or without CORT (1 μM) treatment after pre-miR-155 (LV-miR-155) lentiviral transfection, was measured by real-time PCR. Data are mean ± SEM of six independent experiments; $*p < 0.05$; $**p < 0.01$. (B) Overexpression of miR-155 blocked decreasing of Naive B cells towards iGC B cells differentiation as CORT (1 μM) treatment. FACS staining of GL-7$^+$ Fas$^+$ was analyzed in B220$^+$ B cells in vitro *as described above*. Percentages represent proportion of iGC B cells in each gated population. Representative images were shown. Each symbol represents a cell culture and the horizontal bar corresponds to the media. Asterisks represent statistical differences between groups; $*p < 0.05$; $**p < 0.01$. (C) Overexpression miR-155 blocked FBXO11 mRNA increasing in Naive B cells during its differentiation into iGC B cells through CORT (1 μM) treatment. The CORT treatment or overexpression of miR-155 had no effect on BCL6 mRNA level in B cells. mRNA levels of BCL6 and FBXO11 in abovementioned cells were analyzed by real-time PCR. Data are mean ± SEM of six independent experiments. Asterisks represent statistical differences between groups; $**p < 0.01$. (D) Overexpression of miR-155 blocked FBXO11 expression increasing in Naive B cells during its differentiation into iGC B cells through CORT (1 μM) treatment. The reduction of BCL6 expression in B cells was also significantly blocked. Whole cell extracts from cell cultures were analyzed by Western blotting with antibodies to BCL6, FBXO11 and β-actin. Representative images of three independent experiments were shown. (E) Overexpression of miR-155 significantly prevented the enhanced apoptosis rate in Naive B cells during its differentiation into iGC B cells through CORT (1 μM) treatment. With or without CORT (1 μM) treatment after pre-miR-155 (LV-miR-155) lentiviral transfection, B cell cultures were stained with APC-annexin V for analysis of apoptosis. Representative images were shown. Each symbol represents a cell culture and the horizontal bar corresponds to the media. Asterisks represent statistical differences between groups; $**p < 0.01$.

CORT inhibits GC B cells differentiation. MiR-155 regulates FBXO11 stability which causes the impairment of GC development in response to chronic psychological stress through BCL6 stabilization (Fig. 8).

Chronic emotional stress can make individuals more susceptible to disease due to immunosuppression. Chronic stress can lead to elevated incidence of cell death and of apoptosis or to impaired cell proliferation (Li et al., 2011). The neuroendocrine mechanisms which regulate immune responses have not been unraveled. Numerous in vitro and in vivo studies demonstrated that immune cells are susceptible to glucocorticoids induced by HPA axis activation (Yin et al., 2000). However, the role of GC B cells in stress-mediated immune response inhibition is unexplored. We tested the relevance and underlying mechanisms between chronic psychological stress and GC response. Using an in vivo restraint stress mouse model and an induced GC B cell differentiation model, we demonstrated that chronic psychological stress-induced CORT substantially impaired the GC B cell generation, ultimately incapacitating the GC formation in vivo. Administration of a GR antagonist blocked this impairment in mice, suggesting it is driven by stress-induced activation of the HPA axis. In contrast, other groups have shown that unpredictable chronic mild stress (CMS) exposure markedly altered splenic B cell subset frequency, and glucocorticoid production. These findings positively correlated with the frequency of immature, marginal zone and GC B cells, but negatively correlated with the frequency of follicular B cells (Gurfein et al., 2017). Based upon these observations, we speculated the immunomodulatory impact of stress may be attributed to two pathways, including B cells development and the skewing composition of the B cell compartment.

MiR-155 is induced in human B cells when they engage with an antigen (Yin et al., 2008). MiR-155-deficient mice exhibit impaired GC B cell responses to immunization, including impaired class switching to immunoglobulin G1 (Vigorito et al., 2007). These results suggest that miR-155 plays an active role in cellular immune response (Rodriguez et al., 2007). We explored that miR-155 deficiency in splenic B cells caused by chronic psychological stress; might be involved in GC response impairment. We showed that miR-155 deficiency induced by CORT in B cells lead to decreased numbers of GC B cells and IgG production. Our data suggests that miR-155 targets FBXO11 and regulates its expression, which contributes to GC B cells generation. However, it is well known that miRNAs can regulate several genes affecting the same biological processes (Esquela-Kerscher and Slack, 2006). It has been revealed that additional genes such as PU.1 (Thompson et al., 2011), AID (Teng et al., 2008), SMAD5 (Rai et al., 2010); SHIP1 (Pedersen et al., 2009), and C/EBPbeta (Costinean et al., 2009), are targets of miR-155 too. Additional studies are needed to assess other genes targeted by miR-155 and elucidate its pathogenetic role in GC response.

BCL6 protects GC B cells against apoptosis induced by somatic hypermutation and class-switch recombination associated DNA damage (Ranuncolo et al., 2007). BCL6 has been shown to up-regulate AID via targeting and repressing miR-155 expression (Basso et al., 2012). Accordingly, BCL6 and AID contribute to the GC B cells undergoing SHM and CSR, respectively. However, we observed increased levels of BCL6 and miR-155 in GC B cells. These appeared to be a regulatory circuit of expression between BCL6 and miR-155 as switch for the different stage of GC development, such as centroblasts and centrocytes. The previous study showed that BCL6 was targeted for ubiquitination and subsequent proteasomal degradation by a FBXO11 in DLBCL cell lines (Duan et al., 2012). Thus, we considered the possibility of miR-155 mediated regulation via FBXO1l targeting in GC development. In this study our results indicate that FBXO11 inhibition by miR-155 is associated with higher BCL6 protein levels in splenic B cells and enhanced GC B cell differentiation. These findings demonstrate that FBXO11 inactivation contributes to up-regulation of BCL6 during the GC reaction and is critical for GC development. This is consistent with the recent report which identified a role of FBXO11 in GC homeostasis and lymphomagenesis (Schneider et al., 2016). Interestingly, previous studies raised a question whether phosphorylation of BCL6, induced by MAPK, is involved in the ubiquitin/proteasome degradation process mediated by FBXO11. It might depends on BCR signaling engagement at the different stage of GC B cells development.

The anti-inflammatory effects of glucocorticoids have long been thought to directly inhibit proinflammatory transcription factors including NF-κB. However, glucocorticoids affect the expression of many different miRNAs in multiple cell types, such as miR-27a, miR-223, miR-15b, and miR-16. These miRNAs target the genes involved in proliferation, differentiation, metabolism, and cell survival (Allen and Loh, 2011; Rainer et al., 2009; Chuang et al., 2015). The precise molecular mechanisms of how glucocorticoids regulate miRNAs are not well understood. Recent studies indicate that altered miRNAs are transcriptionally induced by glucocorticoids through binding to GRE in the miRNA promoters (Puimège et al., 2015; Kong et al., 2015), indicating that the GR homodimer can directly bind these sites, potentially leading to altered expression of these miRNAs (Dwivedi et al., 2015).

Our experiments demonstrate that miR-155 could be down-regulated in splenic B cells induced by CORT. It would be interesting to examine how miR-155 is regulated under long-term, elevated CORT, which impairs the GC response. Further studies are needed to determine whether miR-155 expression is regulated through a glucocorticoid receptor mediated by a mechanism of direct DNA-binding, or other activated signaling pathways that regulate miR-155 transcription. It will be critical to elucidate a potential mechanism in immunosuppressive

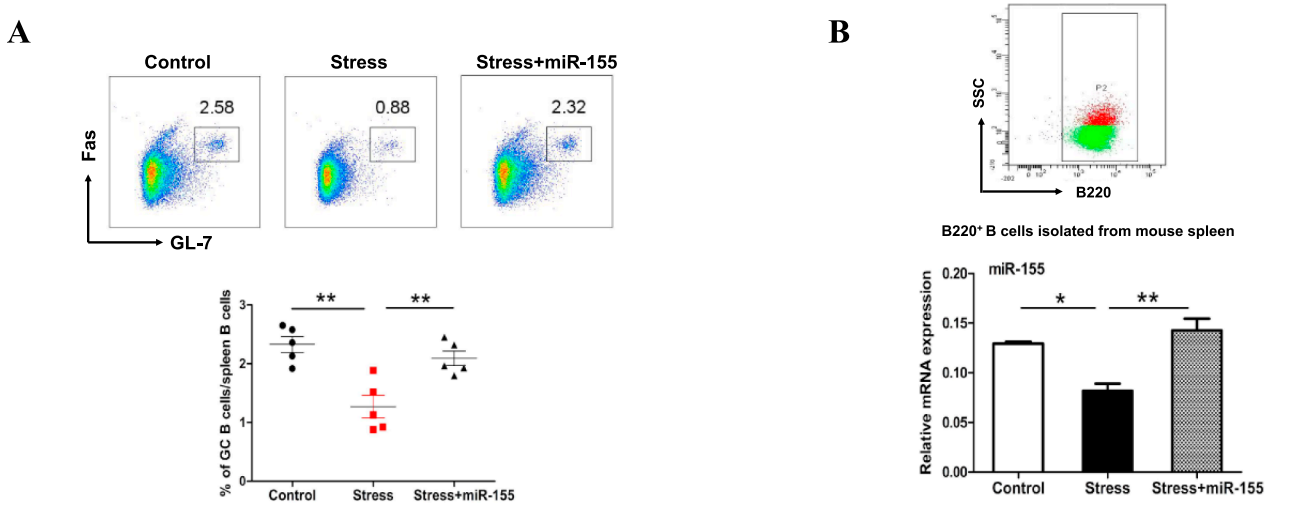

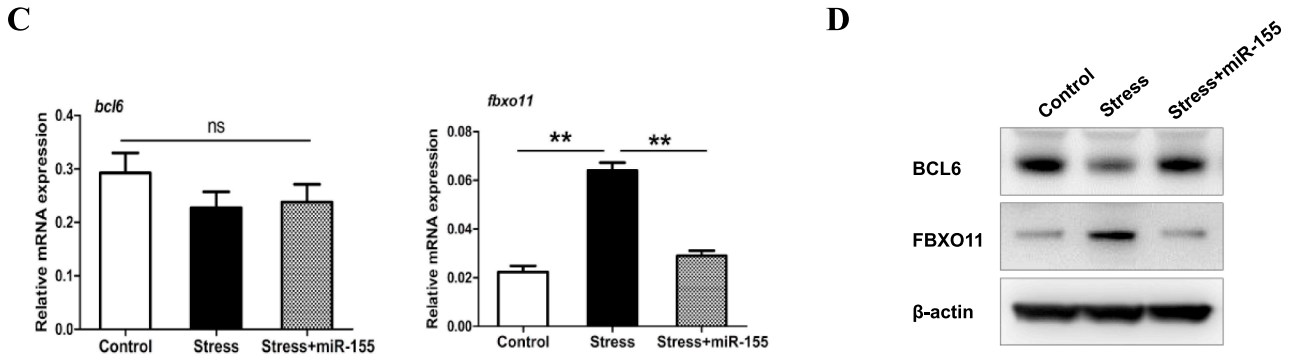

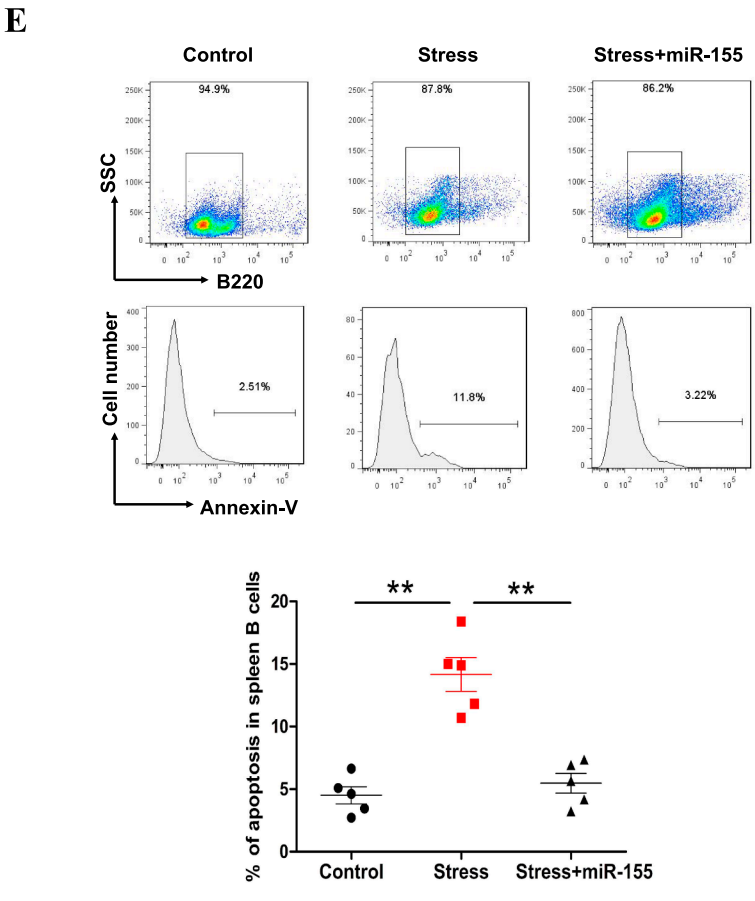

(caption on next page)

Fig.7. Effects of miR-155 overexpression on germinal center response in chronic psychological stress mice. (A) Overexpression of miR-155 blocked GC B cells formation decreasing in mice treated with chronic psychological stress. After lentiviral particles pre-miR-155 (LV-miR-155) injection, mice were immunized with NP-CGG and stressed on days 12. FACS staining of GC B cells (GL-7$^+$ Fas$^+$) were analyzed in splenocytes first gated on B220$^+$ B cells as described in *Materials and Methods*. Representative images were shown. Percentages represent proportion of GC B cells in each gated population. Each symbol represents one mouse and the horizontal bar corresponds to the media. Asterisks represent statistical differences between groups; $^{**}p < 0.01$. (B) Overexpression of miR-155 prevented miR-155 reduction in mice spleen B cells during GC response through chronic psychological stress treatment. Expression of miR-155 in mice spleen B cells were analyzed by real-time PCR. B220$^+$ B cells were isolated from mice splenocytes by FACS sorting with fluorescent-tagged antibody to B220. Data are mean ± SEM of six independent experiments. Asterisks represent statistical differences between groups; $^{*}p < 0.05$; $^{**}p < 0.01$. (C) Overexpression of miR-155 blocked FBXO11 mRNA increasing in mice spleen B cells during GC response through chronic psychological stress treatment. The chronic psychological stress or overexpression of miR-155 had no effect on BCL6 mRNA level in spleen B cells. mRNA levels of BCL6 and FBXO11 in abovementioned mice spleen B cells were analyzed by real-time PCR. B220$^+$ B cells were isolated from mice splenocytes by FACS sorting with fluorescent-tagged antibody to B220. Data are mean ± SEM of six independent experiments. Asterisks represent statistical differences between groups; $^{**}p < 0.01$. (D) Overexpression of miR-155 blocked FBXO11 expression increasing in mice spleen B cells during GC response through chronic psychological stress treatment. The reduction of BCL6 expression in spleen B cells was also significantly blocked and might associated with FBXO11 expression reduction. Whole cell extracts from B220$^+$ B cells in spleens were analyzed by Western blotting with antibodies to BCL6, FBXO11 and β-actin. Representative images of three independent experiments were shown. (E) Overexpression of miR-155 significantly prevented the enhanced apoptosis rate in mice spleen B cells during GC response through chronic psychological stress treatment. Spleen B cells were first gated for B220$^+$ expression, and stained with APC-annexin V for analysis of apoptosis. Representative images were shown. Each symbol represents one mouse and the horizontal bar corresponds to the media. Asterisks represent statistical differences between groups; $^{**}p < 0.01$.

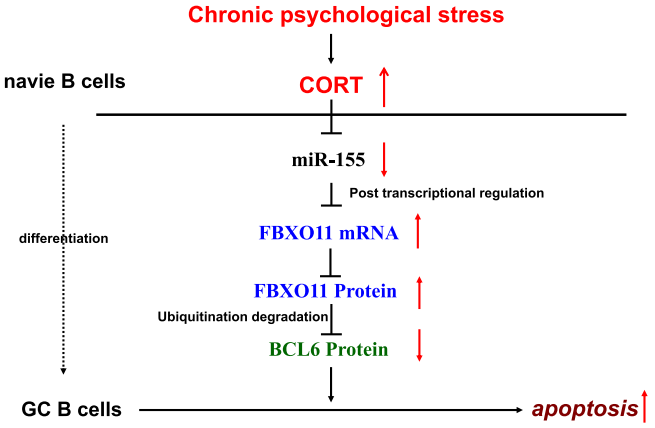

Fig. 8.

diseases induced by chronic psychological stress.

Author contributions

Experiments were conceived and designed by: LZ ZW WS. Experimetns were performed by: WS LL WW. Data were analyzed by: WS YL BY YG. Reagents/materials/analysis tools were contributed by: WS LL XC JH. Wrote the paper: WS LZ.

Funding

The studies were supported by grant for Beijing Municipal Science & Technology Commission, PR China (Z151100004015015), and infectious diseases from National Health and Family Planning Commission, China to XC (2013ZX10003006-003-001).

Competing interests

The authors declare no conflicts of interest.

Appendix A. Supplementary data

Supplementary data to this article can be found online at https://doi.org/10.1016/j.bbi.2018.11.002.

References

Dhabhar, F.S., 2014. Effects of stress on immune function: the good, the bad, and the beautiful. Immunol. Res. 58 (2–3), 193–210.
Aubert, A., 2008. Psychosocial stress, emotions and cytokine-related disorders. Recent Pat Inflamm Allergy Drug Discov. 2 (2), 139–148.
Aberg, K.M., Radek, K.A., Choi, E.H., Kim, D.K., Demerjian, M., et al., 2007. Psychological stress downregulates epidermal antimicrobial peptide expression and increases severity of cutaneous infections in mice. J. Clin. Invest. 117, 3339–3349.
Steelman, A.J., Dean, D.D., Young, C.R., Smith 3rd, R., Prentice, T.W., et al., 2009. Restraint stress modulates virus specific adaptive immunity during acute Theiler's virus infection. Brain Behav. Immun. 23, 830–843.
Neeman, E., Ben-Eliyahu, S., 2013. Surgery and stress promote cancer metastasis: new outlooks on perioperative mediating mechanisms and immune involvement. Brain Behav. Immun. 30 (Suppl), S32–S40.
McEwen, B.S., 2000. The neurobiology of stress: from serendipity to clinical relevance. Brain Res. 886, 172–189.
Haczku, A., Panettieri Jr., R.A., 2010. Social stress and asthma: the role of corticosteroid insensitivity. J. Allergy Clin. Immunol. 125 (3), 550–558.
Webster, J.I., Tonelli, L., Sternberg, E.M., 2002. Neuroendocrine regulation of immunity. Annu. Rev. Immunol. 20, 125–163.
Riccardi, C., Bruscoli, S., Migliorati, G., 2002. Molecular mechanisms of immunomodulatory activity of glucocorticoids. Pharmacol. Res. 45, 361–368.
Truckenmiller, M.E., Bonneau, R.H., Norbury, C.C., 2006. Stress presents a problem for dendritic cells: corticosterone and the fate of MHC class I antigen processing and presentation. Brain Behav. Immun. 20 (3), 210–218.
Elftman, M.D., Norbury, C.C., Bonneau, R.H., Truckenmiller, M.E., 2007. Corticosterone impairs dendritic cell maturation and function. Immunology 122, 279–290.
Igarashi, H., Medina, K.L., Yokota, T., Rossi, M.I., Sakaguchi, N., Comp, P.C., et al., 2005. Early lymphoid progenitors in mouse and man are highly sensitive to glucocorticoids. Int. Immunol. 17, 501–511.
Rosenne, Ella, Sorski, Liat, Shaashua, Lee, 2014. In vivo suppression of NK cell cytotoxicity by stress and surgery in F344 rats: Glucocorticoids have a minor role compared to catecholamines and prostaglandins. Brain Behav. Immun. 37, 207–219.
Suan, D., Sundling, C., Brink, R., 2017. Plasma cell and memory B cell differentiation from the germinal center. Curr. Opin. Immunol. 45, 97–102.
Klein, U., Dalla-Favera, R., 2008. Germinal centres: role in B-cell physiology and malignancy. Nat. Rev. Immunol. 8 (1), 22–33.
Huang, C., Melnick, A., 2015. Mechanisms of action of BCL6 during germinal center B cell development. Sci. China Life Sci. 58 (12), 1226–1232.
Basso, K., Dalla-Favera, R., 2012. Roles of BCL6 in normal and transformed germinal center B cells. Immunol. Rev. 247 (1), 172–183.
Crotty, S., Johnston, R.J., Schoenberger, S.P., 2010. Effectors and memories: Bcl-6 and Blimp-1 in T and B lymphocyte differentiation. Nat. Immunol. 11 (2), 114–120.
Polo, J.M., Ci, W., Licht, J.D., Melnick, A., 2008. Reversible disruption of BCL6 repression complexes by CD40 signaling in normal and malignant B cells. Blood 112 (3), 644–651.
Basso, K., Klein, U., Niu, H., Stolovitzky, G.A., Tu, Y., et al., 2004. Tracking CD40 signaling during germinal center development. Blood 104 (13), 4088–4096.
Saito, M., Gao, J., Basso, K., Kitagawa, Y., Smith, P.M., Bhagat, G., et al., 2007. A signaling pathway mediating downregulation of BCL6 in germinal center B cells is blocked by BCL6 gene alterations in B cell lymphoma. Cancer Cell 12 (3), 280–292.
Phan, R.T., Saito, M., Kitagawa, Y., Means, A.R., Dalla-Favera, R., 2007. Genotoxic stress regulates expression of the protooncogene BCL6 in germinal center B cells. Nat. Immunol. 8 (10), 1132–1139.
Cardozo, T., Pagano, M., 2004. The SCF ubiquitin ligase: insights into a molecular machine. Nat. Rev. Mol. Cell Biol. 5 (9), 739–751.
Duan, S., Cermak, L., Pagan, J.K., Rossi, M., Martinengo, C., di Celle, P.F., et al., 2012. FBXO11 targets BCL6 for degradation and is inactivated in diffuse large B-cell lymphomas. Nature 481 (7379), 90–93.
Huntzinger, E., Izaurralde, E., 2011. Gene silencing by microRNAs: contributions of translational repression and mRNA decay. Nat. Rev. Genet. 12, 99–110.
de Yebenes, V.G., Bartolome-Izquierdo, N., Ramiro, A.R., 2013. Regulation of B-cell development and function by microRNAs. Immunol. Rev. 253, 25–39.
Schmidt, A., Küppers, R., 2014. Role of microRNAs in B cell leukemias and lymphomas. Curr. Mol. Med. 14 (5), 580–597.
Teng, G., Hakimpour, P., Landgraf, P., et al., 2008. MicroRNA-155 is a negative regulator

of activation induced cytidine deaminase. Immunity 28 (5), 621–629.
Nakagawa, Rinako, Leyland, Rebecca, Meyer-Hermann, Michael, Dong, Lu., Turner, Martin, et al., 2016. MicroRNA-155 controls affinity-based selection by protecting c-MYC^{+} B cells from apoptosis. J Clin Invest. 126 (1), 377–388.
Rodriguez, A., Vigorito, E., Clare, S., Warren, M.V., Couttet, P., Soond, D.R., van Dongen, S., Grocock, R.J., Das, P.P., Miska, E.A., et al., 2007. Requirement of bic/microRNA-155 for normal immune function. Science 316, 608–611.
Thai, T.H., Calado, D.P., Casola, S., Ansel, K.M., Xiao, C., Xue, Y., Murphy, A., Frendewey, D., Valenzuela, D., Kutok, J.L., et al., 2007. Regulation of the germinal center response by microRNA-155. Science 316, 604–608.
Nojima, T., Haniuda, K., Moutai, T., Matsudaira, M., Mizokawa, S., Shiratori, I., Azuma, T., Kitamura, D., 2011. In-vitro derived germinal centre B cells differentially generate memory B or plasma cells in vivo. Nat. Commun. 2, 465.
Li, H., Chen, L., Zhang, Y., Lesage, G., Zhang, Y., Wu, Y., Hanley, G., Sun, S., Yin, D., 2011. Chronic stress promotes lymphocyte reduction through TLR2 mediated PI3K signaling in a beta-arrestin 2 dependent manner. J. Neuroimmunol. 233 (1–2), 73–79.
Yin, D., Tuthill, D., Mufson, R.A., Shi, Y., 2000. Chronic restraint stress promotes lymphocyte apoptosis by modulating CD95 expression. J. Exp. Med. 191 (8), 1423–1428.
Gurfein, Hasdemir, Milush, J.M., Touma, C., Palme, R., Nixon, D.F., Darcel, N., Hecht, F.M., Bhargava, A., 2017. Enriched environment and stress exposure influence splenic B lymphocyte composition. PLoS One 12 (7), e0180771.
Yin, Q., Wang, X., McBride, J., Fewell, C., Flemington, E., 2008. B-cell receptor activation induces BIC/miR-155 expression through a conserved AP-1 element. J. Biol. Chem. 283 (5), 2654–2662.
Vigorito, E., Perks, K.L., Abreu-Goodger, C., et al., 2007. microRNA-155 regulates the generation of immunoglobulin class-switched plasma cells. Immunity 27 (6), 847–859.
Esquela-Kerscher, A., Slack, F.J., 2006. Oncomirs: microRNAs with a role in cancer. Nat. Rev. Cancer 6 (4), 259–269.
Thompson, R.C., Herscovitch, M., Zhao, I., Ford, T.J., Gilmore, T.D., 2011. NF-kappaB down-regulates expression of the B-lymphoma marker CD10 through a miR-155/PU.1 pathway. J. Biol. Chem. 286 (3), 1675–1682.
Rai, D., Kim, S.W., McKeller, M.R., Dahia, P.L., Aguiar, R.C., 2010. Targeting of SMAD5 links microRNA-155 to the TGF-beta pathway and lymphomagenesis. Proc. Natl. Acad. Sci. USA 107 (7), 3111–3116.
Pedersen, I.M., Otero, D., Kao, E., et al., 2009. Onco-miR-155 targets SHIP1 to promote TNFalpha-dependent growth of B cell lymphomas. EMBO Mol. Med. 1 (5), 288–295.
Costinean, S., Sandhu, S.K., Pedersen, I.M., et al., 2009. Src homology 2 domain-containing inositol-5-phosphatase and CCAAT enhancer-binding protein beta are targeted by miR-155 in B cells of Emicro-MiR-155 transgenic mice. Blood 114 (7), 1374–1382.
Ranuncolo, S.M., Polo, J.M., Dierov, J., Singer, M., Kuo, T., Greally, J., Green, R., Carroll, M., Melnick, A., 2007. Bcl-6 mediates the germinal center B cell phenotype and lymphomagenesis through transcriptional repression of the DNA-damage sensor ATR. Nat. Immunol. 8 (7), 705–714.
Basso, K., Schneider, C., Shen, Q., Holmes, A.B., Setty, M., Leslie, C., Dalla-Favera, R., 2012. BCL6 positively regulates AID and germinal center gene expression via repression of miR-155. J. Exp. Med. 209 (13), 2455–2465.
Schneider, C., Kon, N., Amadori, L., Shen, Q., Schwartz, F.H., et al., 2016. FBXO11 inactivation leads to abnormal germinal-center formation and lymphoproliferative disease. Blood 128 (5), 660–666.
Allen, D.L., Loh, A.S., 2011. Posttranscriptional mechanisms involving microRNA-27a and b contribute to fast-specific and glucocorticoid-mediated myostatin expression in skeletal muscle. Am. J. Physiol. Cell Physiol. 300 (1), C124–C137.
Rainer, J., Ploner, C., Jesacher, S., Ploner, A., Eduardoff, M., Mansha, M., Wasim, M., et al., 2009. Glucocorticoid-regulated microRNAs and mirtrons in acute lymphoblastic leukemia. Leukemia 23, 746–752.
Chuang, T.D., Pearce, W.J., Khorram, O., 2015. miR-29c induction contributes to downregulation of vascular extracellular matrix proteins by glucocorticoids. Am. J. Physiol. Cell Physiol. 309 (2), C117–C125.
Puimège, L., Van Hauwermeiren, F., Steeland, S., Van Ryckeghem, S., Vandewalle, J., Lodens, S., et al., 2015. Glucocorticoid-induced microRNA-511 protects against TNF by down-regulating TNFR1. EMBO Mol. Med. 7 (8), 1004–1017.
Kong, X., Yu, J., Bi, J., Qi, H., Di, W., Wu, L., Wang, L., Zha, J., et al., 2015. Glucocorticoids transcriptionally regulate miR-27b expression promoting body fat accumulation via suppressing the browning of white adipose tissue. Diabetes 64 (2), 393–404.
Dwivedi, Y., Roy, B., Lugli, G., Rizavi, H., Zhang, H., Smalheiser, N.R., 2015. Chronic corticosterone-mediated dysregulation of microRNA network in prefrontal cortex of rats: relevance to depression pathophysiology. Transl. Psychiatry 5, e682.